Supplemental Figures and Tables

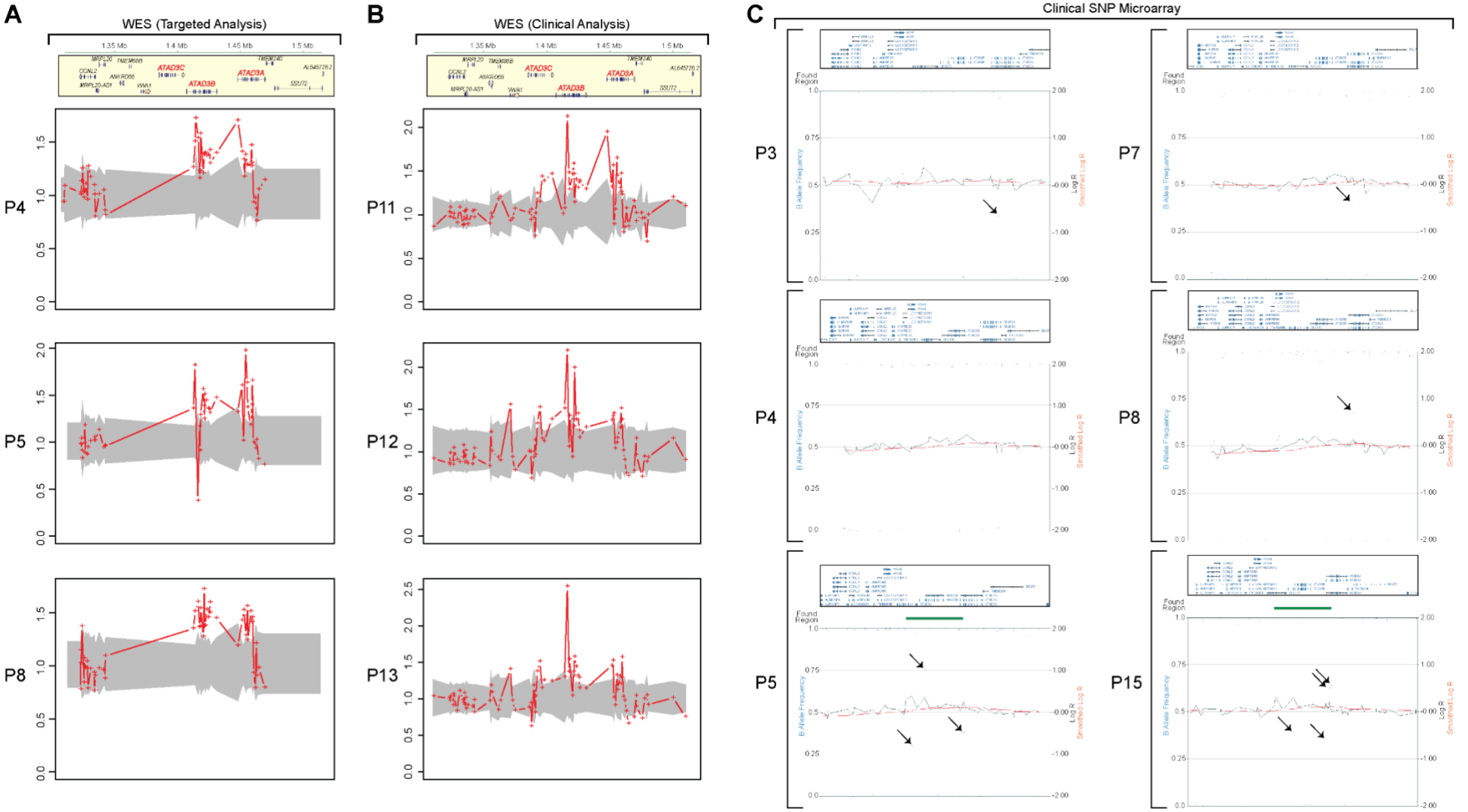

Supplemental Figure 1. Additional ExomeDepth images and chromosomal SNP microarray analyses for *ATAD3dup* patients, related to **Figure 1**. ExomeDepth analysis across the *ATAD3* locus in patients from the cohort not shown in **Figure 1C** plotted as the ratio of the observed versus expected read depth. Samples analyzed were subjected to whole exome sequencing with either **A)** targeted analysis of mitochondrial genes or **B)** clinical analysis. Shaded grey areas indicate 95% confidence interval across the matched reference set. **C)** Patient gDNA samples were analyzed using the Illumina Infinium Global Screening Array-24 platform. Graphs of the region encompassing the *ATAD3* locus indicate B allele frequency (left axis, blue), LogR (right axis, black line) and smoothed LogR (right axis, orange line). Incidences where the B allele frequency values fall between 0, 0.5 and 1 are indicative of allelic imbalances (i.e. 0 = no B allele, 0.5 = one B allele, 1 = two B alleles), and are indicated by arrows. The *ATAD3* duplication was identified only in patients P5 and P15 (green bars).

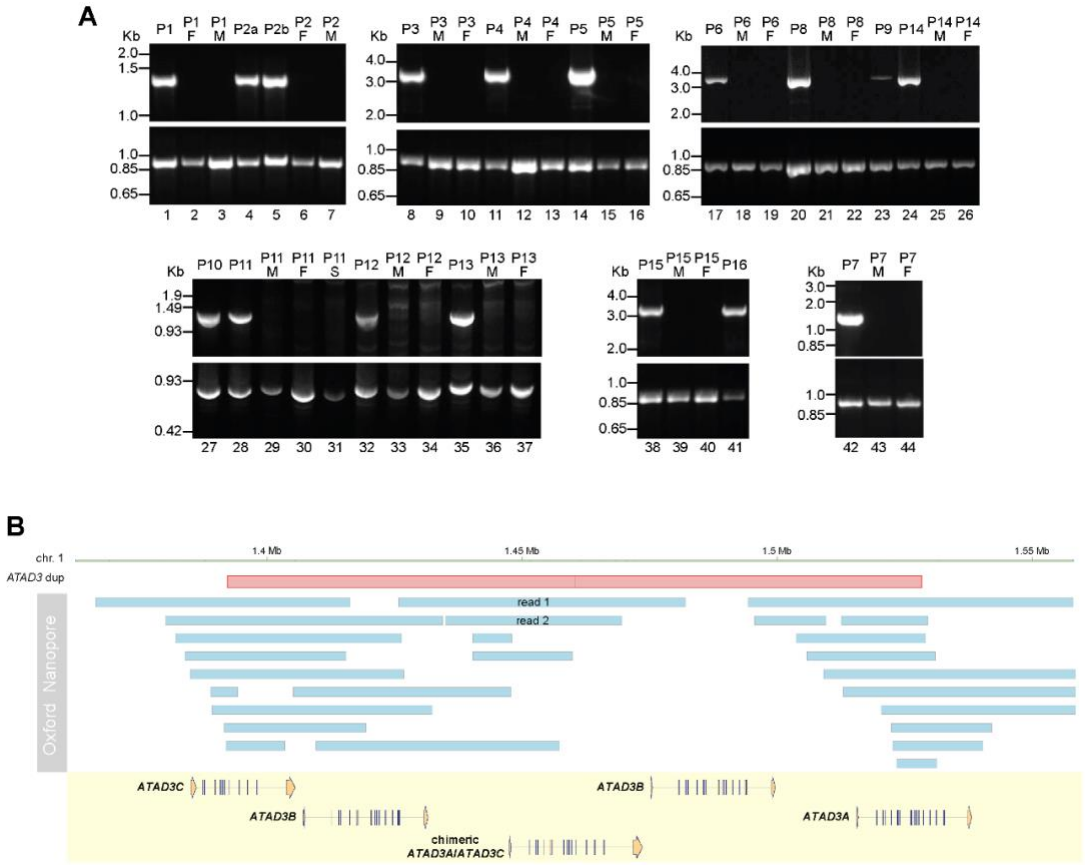

Supplemental Figure 2. Parental DNA analysis and *ATAD3dup* confirmation by long read DNA sequencing, **related to Figure 1** and **2**. **A)** The duplication breakpoint in *ATAD3A*/*ATAD3C* was analyzed by PCR of gDNA from patients and family members (M, mother; F, father; S, sibling), using flanking primers located in *ATAD3A* and *ATAD3C* (see **Supplemental Table 4**). Breakpoint PCRs (top panels) of patients and family members performed using either primers OT865 and OT866 (lanes 1-7 and 27-37), OT864 and OT865 (lanes 8-26 and 38-41), or OT873 and OT879 (lanes 42-44) indicated the *ATAD3* duplication was *de novo* in all cases with available parental samples for analysis. To control for sample integrity, a control gDNA PCR of a region in *ATAD3C* was performed using primers OT583 and OT866 (lower panels). **B)** gDNA prepared from P3 fibroblasts was subjected to long read DNA sequencing on an Oxford Nanopore Technologies (ONT) PromethION flow cell (2.71 M reads, 35.18 Gb, N50 = 26.47 Kb). ONT reads (blue boxes) were aligned to an artificial chromosome 1 created to encode the predicted *ATAD3* tandem duplication (duplicated region, red boxes). Two reads spanning the *ATAD3A*/*ATAD3C* breakpoint were identified (read 1, 56.215 Kb; read 2, 34.608 Kb).

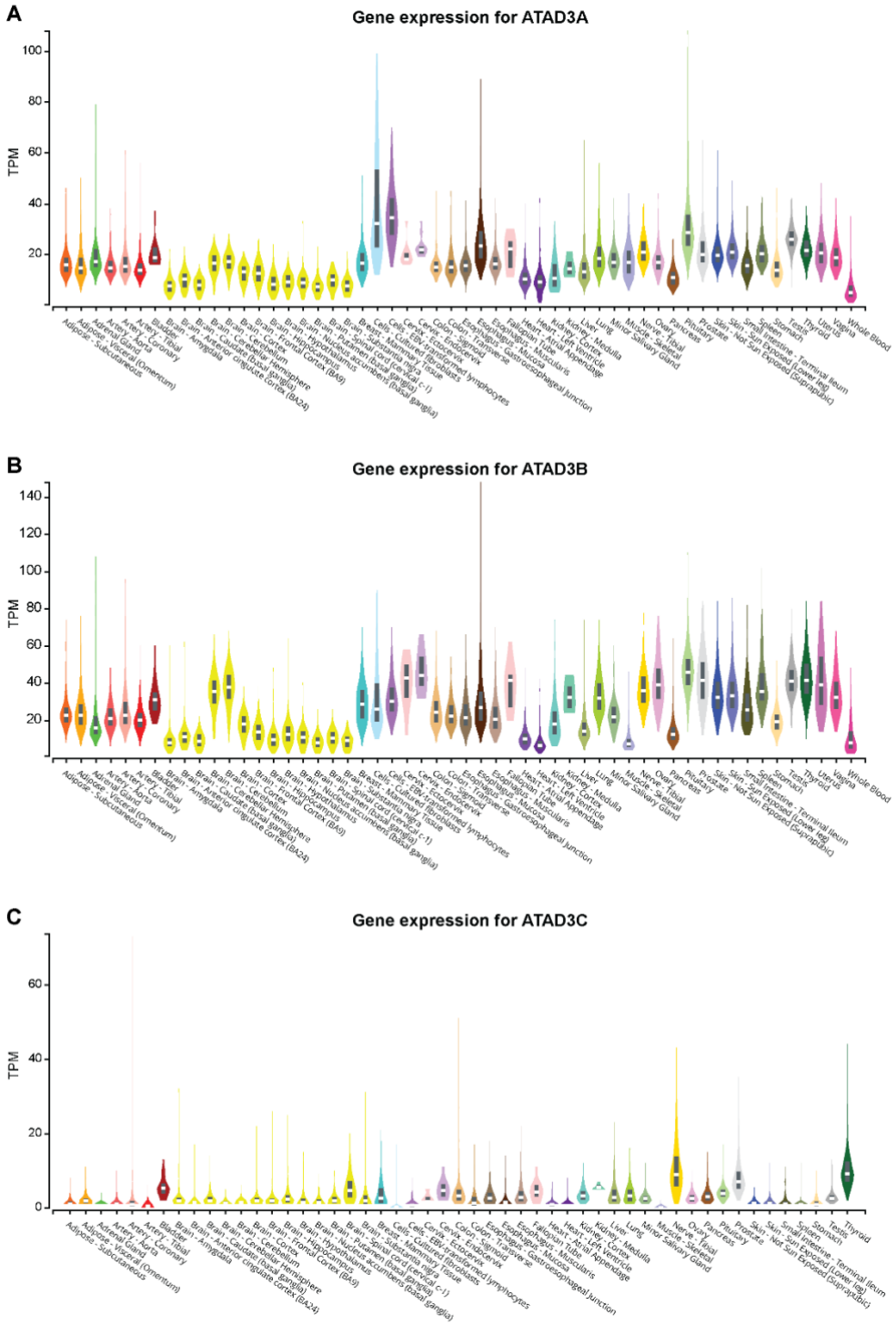

Supplemental Figure 3. *ATAD3A*, *ATAD3B* and *ATAD3C* transcript expression across tissues, related to **Figure 3**. Gene expression data across all available tissues expressed as Transcripts Per Million (TPM) obtained from the GTEx Portal for **A)** *ATAD3A* (ENSG00000197785.13), **B)** *ATAD3B* (ENSG00000160072.19) and **C)** *ATAD3C* (ENSG00000215915.9). The data used for the analyses described in this manuscript were obtained from the GTEx Portal on November 28, 2019.

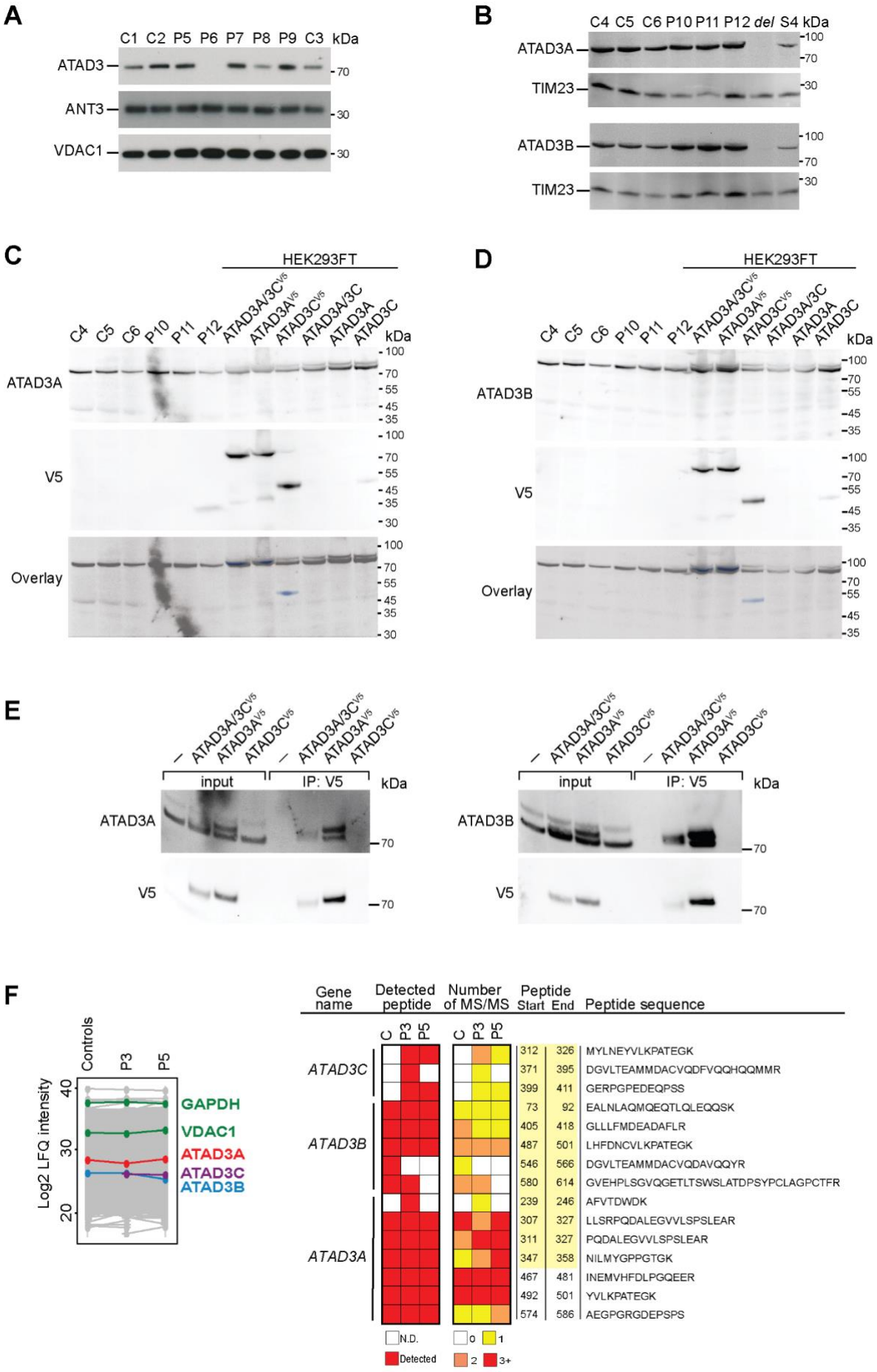
A
C1 C2 P5 P6 P7 P8 P9 C3 kDa
ATAD3
ANT3
VDAC1
70
30
30
B
C4 C5 C6 P10 P11 P12 del S4 kDa
ATAD3A
TIM23
ATAD3B
TIM23
100
70
30
100
70
30
C
HEK293FT
C4 C5 C6 P10 P11 P12 ATAD3A/3C^V5 ATAD3A^V5 ATAD3C^V5 ATAD3A/3C ATAD3A ATAD3C kDa
ATAD3A
V5
Overlay
100 70 55 45 35
100 70 55 45 35 30
100 70 55 45 35 30
D
HEK293FT
C4 C5 C6 P10 P11 P12 ATAD3A/3C^V5 ATAD3A^V5 ATAD3C^V5 ATAD3A/3C ATAD3A ATAD3C kDa
ATAD3B
V5
Overlay
100 70 55 45 35
100 70 55 45 35
100 70 55 45 35
E
– ATAD3A/3C^V5 ATAD3A^V5 ATAD3C^V5 – ATAD3A/3C^V5 ATAD3A^V5 ATAD3C^V5
input
IP: V5
kDa
ATAD3A
V5
70
70
– ATAD3A/3C^V5 ATAD3A^V5 ATAD3C^V5 – ATAD3A/3C^V5 ATAD3A^V5 ATAD3C^V5
input
IP: V5
kDa
ATAD3B
V5
70
70
F
Controls
P3
P5
Log2 LFQ intensity
40
30
20
GAPDH
VDAC1
ATAD3A
ATAD3C
ATAD3B
Gene name
Detected peptide
Number of MS/MS
Peptide Start
End
Peptide sequence
C P3 P5
C P3 P5
ATAD3C
ATAD3B
ATAD3A
312 326 MYLNEYVLKPATEGK
371 395 DGVLTEAMMDACVQDFVQQHQQMMR
399 411 GERPGPEDEQPSS
73 92 EALNLAQMQEQTLQLEQQSK
405 418 GLLLFMDEADAFLR
487 501 LHFDNCVLKPATEGK
546 566 DGVLTEAMMDACVQDAVQQYR
580 614 GVEHPLSGVQGETLTSWSLATDPSYPCLAGPCTFR
239 246 AFVTDWDK
307 327 LLSRPQDALEGVVLSPSLEAR
311 327 PQDALEGVVLSPSLEAR
347 358 NILMYGPPGTGK
467 481 INEMVHFDLPGQEER
492 501 YVLKPATEGK
574 586 AEGPGRGDEPSPS
N.D.
Detected
0
1
2
3+

Supplemental Figure 4. ATAD3 immunoblotting and quantitative proteomics, related to **Figure 3**. **A)** Total heart lysates from controls and patients (2 µg) analyzed by SDS-PAGE and western blotting with a pan anti-ATAD3 antibody (generated against a.a. 44-247 of ATAD3B[28]), and with loading controls VDAC1 (porin) and ANT3 (repeated from **Figure 3G**). Sample integrity issues were noted for P6. **B)** Mitochondrial extracts from control and patient fibroblasts (20 µg) analyzed by SDS-PAGE and western blotting with commercially available anti-ATAD3A and anti-ATAD3B (Abnova) antibodies. Antibodies for ATAD3A and ATAD3B were generated against full-length human proteins (ATAD3A, 586 a.a.; ATAD3B, 648 a.a). For comparison, samples from *ATAD3*del patients (*del,* unpublished; and S4[19]) analyzed alongside controls and *ATAD3*dup patient samples. **C, D)** Mitochondrial extracts from control and patient fibroblasts (20 µg) analyzed by SDS-PAGE alongside HEK293FT cells expressing full-length ATAD3A, ATAD3C, or chimeric ATAD3A/3C with or without a V5-tag. Western blotting performed using commercially available antibodies against the V5-tag and **C)** anti-ATAD3A (Abnova) or **D)** anti-ATAD3B (Abnova) and an image overlay performed (blue, anti-V5) to confirm antibody specificity. **E)** HEK293FT cells expressing full-length V5-tagged ATAD3A, ATAD3C, or chimeric ATAD3A/3C were subjected to co-immunoprecipitation with anti-V5, then separated on SDS-PAGE and analyzed by immunoblotting with anti-V5 and anti-ATAD3A (Abnova) or anti-ATAD3B (Abnova) antibodies. ATAD3C^{V5} is not visible due to extended electrophoresis time to separate higher molecular weight proteins. **F)** Label-free quantitative proteomics (LFQ) performed on skin fibroblasts from controls (n=3) and *ATAD3*dup patients P3 and P5 (each in duplicate). Control samples and patient replicates were pooled prior to MS/MS analysis preventing evaluation of individual control and sample variation. A different set of control fibroblast lines were used in comparison to **Figure 3E-F.** Using peptides unique to each protein, the relative levels of ATAD3A, ATAD3B and ATAD3C proteins in each sample were compared (left panel), alongside the levels of cytosolic (GAPDH) and mitochondrial (VDAC1) marker proteins. Unique ATAD3A and ATAD3B peptides (right panel) and the sequence information were plotted according to their presence, as well as the number of MS/MS

spectra observed. The yellow box indicates the peptides encoded within the duplicated *ATAD3* region. N.D., not detected.

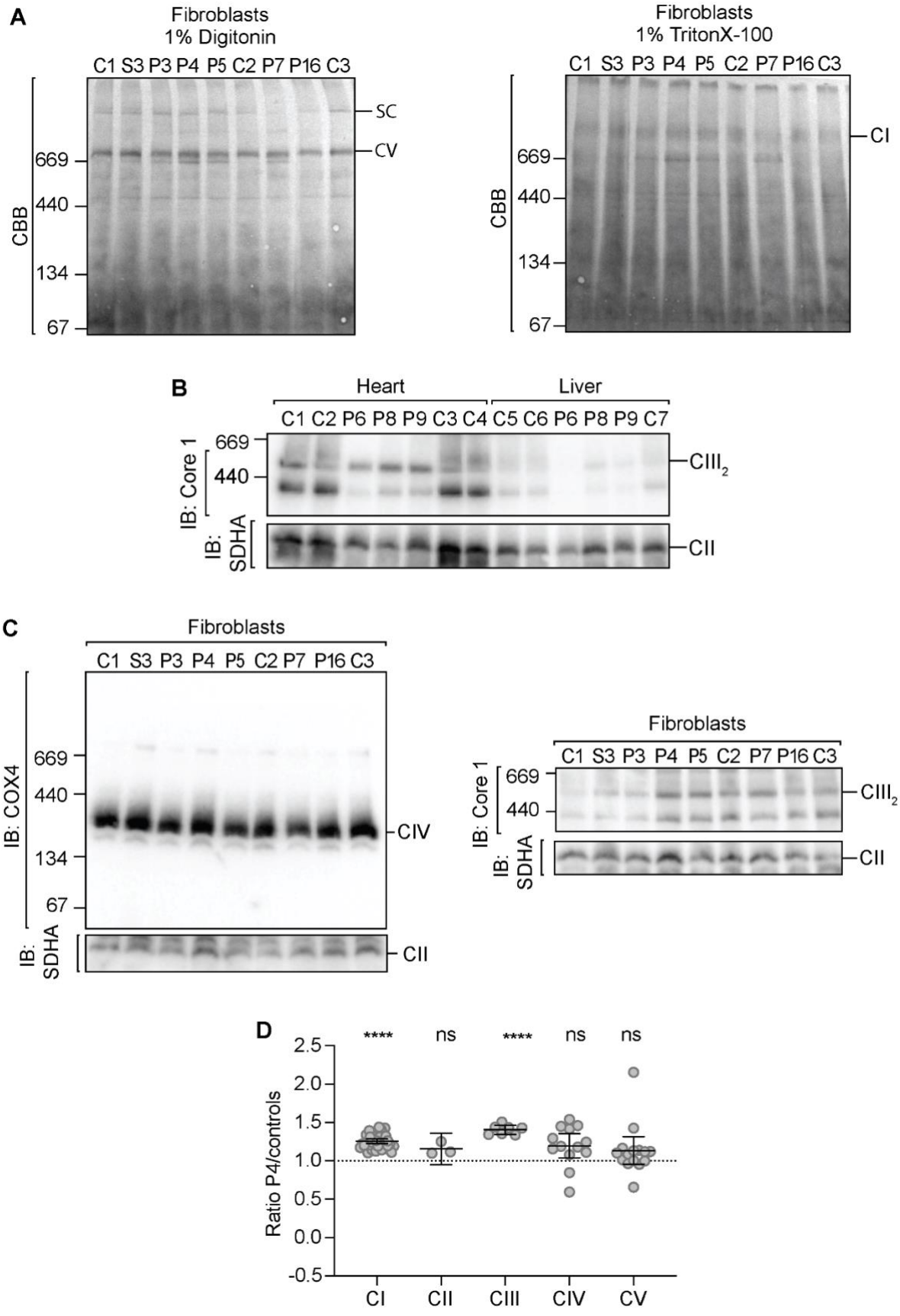
A
Fibroblasts
1% Digitonin
C1 S3 P3 P4 P5 C2 P7 P16 C3
CBB
669
440
134
67
SC
CV
Fibroblasts
1% TritonX-100
C1 S3 P3 P4 P5 C2 P7 P16 C3
CBB
669
440
134
67
CI
B
Heart
Liver
C1 C2 P6 P8 P9 C3 C4 C5 C6 P6 P8 P9 C7
IB: Core 1
669
440
CIII2
IB: SDHA
CII
C
Fibroblasts
C1 S3 P3 P4 P5 C2 P7 P16 C3
IB: COX4
669
440
134
67
CIV
IB: SDHA
CII
Fibroblasts
C1 S3 P3 P4 P5 C2 P7 P16 C3
IB: Core 1
669
440
CIII2
IB: SDHA
CII
D
****
ns
****
ns
ns
Ratio P4/controls
2.5
2.0
1.5
1.0
0.5
0.0
-0.5
CI
CII
CIII
CIV
CV

Supplemental Figure 5. Additional OXPHOS complex analyses in *ATAD3*dup patients, related to **Figure 4**. **A)** Coomassie brilliant blue (CBB) staining of Blue Native (BN)-PAGE gels from **Figure 4C** (fibroblast mitochondria solubilized in 1% digitonin) and **Figure 4F** (fibroblast mitochondria solubilized in 1% TX-100). SC, supercomplex. **B)** Mitochondria isolated from control and patient heart and liver biopsies were solubilized in 1% Triton X-100 and subjected to BN-PAGE and analysis by repeat immunoblotting of **Figure 4E** membrane for OXPHOS complex III (anti-Core1). For comparison, immunoblot for complex II (anti-SDHA) is shown again. **C)** Mitochondria isolated from control and patient fibroblasts were solubilized in 1% Triton X-100 and subjected to BN-PAGE and analysis of OXPHOS complex IV by immunoblotting (anti-COX4), in comparison to OXPHOS complex II (anti-SDHA). As well, analysis of CIII (anti-Core1) was performed by repeat immunoblotting of **Figure 4F** membrane; the immunoblot for complex II (anti-SDHA) is shown again for comparison. **D)** Analysis of OXPHOS protein levels determined from LFQ proteomics for controls (n=4) and the *ATAD3*dup patient P4 (in triplicate). Plot shows mean ratio (controls versus P4) with 95% confidence interval for each complex. Proteins were filtered to have a minimum of two peptides and each dot represents a single protein. Significance was determined by a two-tailed ratio paired t-test performed on mean LFQ intensities between groups (controls and P4) using built-in functions in Prism 8 (v.8.3.1). **** = $p<0.0001$ significance from two-tailed ratio t-test.

Supplemental Table 1. Case Reports, related to **Figures 1** and **2**.

P1

The female patient was born at 37+3 weeks gestation by caesarean section with Apgar scores of 7 and 9 at 1 and 5 minutes, respectively. The pregnancy was uncomplicated and the parents were of non-consanguineous European (Dutch) background. Her birth weight was 2250 gm (2.3^{th} - 10^{th} percentiles). The hemoglobin was low (7.3 mmol/l) and she had an ophthalmic inspection showing bilateral cataracts. Feeding was problematic and she was hypotonic from birth. The first brain ultrasound showed hyperechogenic basal ganglia. She had progressive hypotonia and developed respiratory insufficiency at 14 days of life, with ventilation commencing at day 16. Liver function tests showed increased gamma-glutamyl transferase (GGT) and alkaline phosphatase. Urine metabolic screening showed elevated levels of tiglylglycine, propionylglycine, isobutyrylglycine, isovalerylglycine and 3-methylcrotonylglycine plus elevated alanine. Cardiac ultrasound showed hypertrophic cardiomyopathy, with some pericardial fluid and pulmonary hypertension. Because of a potential underlying infection, she was treated with antibiotics (amoxicillin and gentamicin) and an antiviral drug (acyclovir), with treatment stopped upon negative tests. Electroencephalogram (EEG) showed a burst-suppression pattern without epileptic seizures. Magnetic resonance imaging (MRI) of the brain showed extensive T2-hyperintensity and striking swelling of the cerebral white matter, mild pontocerebellar hypoplasia, bilateral subependymal pseudocysts, T1-hyperintensity consistent with calcium deposits in the basal ganglia and a lactate peak in magnetic resonance spectroscopy (MRS). Respiratory chain enzyme measurements in skeletal muscle and skin fibroblasts were all within reference limits. She deteriorated further clinically and died on the 38^{th} day of life after withdrawal of artificial ventilation.

P2a and P2b

Identical twin brothers were born at 37 weeks gestation by lower segment caesarean section for failure to progress following an otherwise uncomplicated pregnancy to unrelated parents of European (Australian) descent.

P2a: Apgar scores were 2 and 6 at 1 and 5 minutes, respectively. Birth weight was 2575 gm (10^{th} – 25^{th} percentiles). He initially required some supplemental oxygen for a short period. On day 3, he began having apneas and was noted to be hypotonic. He was transferred from the peripheral birth hospital to a tertiary center. He went on to develop a progressive neonatal encephalopathy (burst suppression pattern on EEG), and was found to have lactic acidosis, with blood lactate persistently over 5 mmol/L. Urine organic acids showed a slight increase in methylmalonate and methylcitrate with normal levels of lactate and 3-methylglutaconic acid. He went onto CPAP on day 4 and required intubation, ventilation and inotrope support by day 5. Mechanical ventilation was not difficult, with pO2 well maintained. However, lactic acidemia persisted, and required bicarbonate correction at least once. He was also noted to have hypertrophic cardiomyopathy and quite prominent corneal clouding. He continued to deteriorate despite maximal resuscitation and died on day 6 of life. Normal investigations included plasma amino acids, uric acid, serum transferrin isoforms, plasma very long chain fatty acids, urine glycosaminoglycans, amino acids (including S-sulfocysteine), organic acids, creatine and guanidino-acetate, and white blood cell lysosomal enzymes. CSF glycine was 20 mmol/L (normal range; NR 4 – 14), but plasma glycine was 106 mmol/L (NR 160-527). The karyotype was confirmed as 46XY.

Skeletal muscle and liver were collected within the first few hours after death for respiratory chain enzymology, which was unremarkable, with complex I at the lower end of the reference range in both tissues at 52% and 50% residual activity relative to citrate synthase, respectively. At autopsy, he was found to have very similar features to his brother, with bilateral dense corneal clouding, pleural effusions, hypertrophic cardiomyopathy (weight 28.4 gm; NR 17 +/- 2.8) with thickening of the right

(8 mm) and left (9 mm) ventricular walls, patchy hepatic necrosis, widespread gliosis and microglial activation with some neuronal loss in the brain consistent with energy failure, with no other apparent structural abnormalities. Sanger sequencing of the *AGK* gene and testing for 22 "common" mitochondrial DNA (mtDNA) and 3 common *POLG* mutations was negative. In addition, mtDNA depletion testing of liver DNA was normal.

P2b: Apgar scores were 4 and 7 at 1 and 5 minutes, respectively. Birth weight was 2530 gm (10^{th} – 25^{th} percentiles). Within the first 24 hours of life he became lethargic, fed poorly and was noted to be hypotonic. Cardiomegaly was noted on chest X-ray at this time. Hypothermia ensued and he became encephalopathic. Corneal clouding was noted, and he was also found to have bilateral fixed flexion deformities of the elbows and knees. He became apneic and bradycardic on day 5, but despite vigorous attempts at resuscitation he succumbed at the peripheral birth hospital. Persistent lactic acidosis was noted. Normal investigations included urine glycosaminoglycans, creatine, guanidino-acetate and amino acids, plasma very long chain fatty acids, and serum transferrin isoforms. Urine organic acids showed a normal lactate, but slight elevations of methylmalonic acid and methylcitrate. The karyotype was confirmed as 46XY. Bilateral dense corneal clouding was noted as well as bilateral pleural effusions, and hypertrophic cardiomyopathy (weight 31.3 gm; NR 17 +/- 2.8), with thickening of the right (6.5-7.0 mm) and left (7.0-7.5 mm) ventricular walls, and the interventricular septum (8.0 mm). Neuropathology showed microglial activation and gliosis with some neuronal loss and occasional necrotic neurons in the brainstem, cerebellar dentate nucleus, basal ganglia, thalamus, and subiculum. Apart from some pallor with occasional necrotic cells, the cerebral white matter was relatively spared. Full mtDNA sequencing performed through WGS was normal.

P3

The male infant, the third child to a non-consanguineous European (Australian) couple was born at 38 weeks gestation by elective caesarean section without labor after a pregnancy complicated by intra-uterine growth retardation (IUGR) and right ventricular hypertrophy noted on a fetal echocardiogram at 38 weeks gestation. Birth weight was 2339 gm (3rd percentile). Apgar scores were 5, 3 and 7 at 1, 5 and 10 minutes, respectively. He was electively intubated and ventilated following the onset of respiratory distress and transferred to a neonatal intensive care unit. A postnatal echocardiogram showed non compaction cardiomyopathy with marked hypertrophy of the apex of the right ventricle. A chest X-ray showed cardiac enlargement. He had bilateral corneal opacification. He was extubated but had recurrent apneic episodes and required continuous positive pressure ventilation. Serial echocardiograms revealed biventricular dysfunction, left ventricular dilatation and pulmonary hypertension. The ejection fraction deteriorated to 30% on day 5 and was treated with captopril, digoxin and frusemide with improvement to 50-60% on day 7. Abnormal posturing was noted with extension of the limbs and neck arching. An EEG showed a normal background interspersed with periods of burst suppression but no electrical seizure activity. Brain MRI on day 8 showed diffuse T2-hyperintensity and mild swelling of the cerebral white matter and dilated inferior horns of the lateral ventricles, particularly on the right. There were bilateral subependymal pseudocysts. There was a high lactate peak on MRS. Urinary organic acids analysis showed a slight increase in lactate and methylglutaconate. Blood lactates were persistently elevated. On day 9 he had increased work of breathing with gasping breaths, desaturation and bradycardia requiring re-intubation and ventilation. He was treated for sepsis after a septic workup with intravenous antibiotics, but blood cultures were negative. A clinical decision was made with the parents for palliation. The baby died on day 9 after extubation. Skeletal muscle, liver and skin biopsies were collected 2 hours postmortem for mitochondrial respiratory chain enzymology. Complex I activity in liver was low relative to citrate synthase (24% of control mean) while muscle results were

unremarkable. mtDNA deletion and duplication studies, and full mtDNA sequencing performed through WGS, were normal. A routine chromosome microarray was normal.

P4

The patient's mother was a 22-year-old primigravid patient who had normal / low risk first and second trimester screening. The female infant was born by an elective caesarean section at 39 weeks gestation for breech presentation and concerns about IUGR. Despite her mother not laboring, the liquor contained meconium. She was growth restricted with a birth weight of 1984 gm (< 3rd percentile) and a head circumference of 30.5 cm (< 3rd percentile). She was "unexpectedly depressed" at delivery required bag and mask ventilation with oxygen for 5 minutes for resuscitation. Her Apgar scores were 1, 7 and 8 at 1, 5 and 10 minutes, respectively. On admission to the nursery, hip flexion deformities were noted and she had redundant skin around the neck but was not otherwise dysmorphic. An initial milk feed was given. Hypoglycemia was noted 4 hours after birth (1.4 mmol/L) and resolved with a 12.5% dextrose infusion. This was associated with a compensated metabolic acidosis with an elevated capillary blood lactate of 7 mmol/L that did not respond to intravenous sodium bicarbonate. The differential diagnosis considered was asphyxia versus a metabolic disorder and intravenous antibiotics were commenced for potential sepsis. Cranial ultrasound showed echogenicity of the left lenticulostriate region and of the basal ganglia bilaterally. Echocardiogram showed normal anatomy with borderline to low ventricular contractility. The baby was mildly anemic (hemoglobin 122 g/L) with a normal white cell count and differential and platelet clumping prevented a platelet count. C-reactive protein (CRP) was not elevated and blood culture was negative at 48 hours. Clotting profile was normal. Urea and electrolytes were normal. Creatinine was elevated (0.09 mmol/L, 3 times upper limit). GGT was elevated (4 times upper limit) but liver function was otherwise normal although serum albumin was borderline (23 g/L). The metabolic physicians were consulted at 36 hours of age and intravenous carnitine, oral biotin and riboflavin were added. Total parenteral nutrition (TPN) was withdrawn. Small milk feeds

were re-introduced at 48 hours. Urine and blood spot amino acids and acylcarnitines, an infective disease serology screen and blood hexose-1-phosphate uridyl transferase activity were all normal / negative. The urine organic acid profile was consistent with neonatal lactic acidosis. Paired CSF glucose, pyruvate and lactate levels were planned, but deferred. Lactic acidosis persisted (peak 21 mmol/L) despite medical intervention and fluid management. At 68 hours of age, she became poorly perfused with intermittent respiratory effort needing intubation, ventilation, volume expanders, inotrope infusions and further sodium bicarbonate corrections for significant metabolic acidosis (pH 7.0, HCO_3 10 mmol/L, base excess -20 mmol/L, lactate 25 mmol/L). During resuscitation she had tonic-clonic limb movements associated with apnea and was loaded with phenobarbitone for seizures. She was transferred to a tertiary pediatric center for further investigation of a likely mitochondrial disorder. Following transfer, while ventilated, she continued to have seizures despite being loaded with phenytoin. MRI brain scan showed diffuse mildly increased T2 signal in the white matter of both cerebral hemispheres with mild swelling. The cortex, basal ganglia, cerebellum and brainstem appeared normal with appropriate myelination for gestation. Limited MRS from the frontal white matter demonstrated an elevated lactate peak with a small N-acetylaspartate (NAA) peak. Her lactic acidosis persisted (pH 7.18 to 7.25; lactate 18.9 mmol/L -> 15.9 mmol/L) despite medical management. Electrolyte studies showed mild hypernatremia (Na^+ 147 mmol/L). Liver function tests showed persistent elevation of GGT and significant hypoalbuminemia (albumin 14 g/L). She deteriorated over the next 24 hours with multiple seizure events and increasing ventilatory requirements. In consultation with her parents, care was withdrawn and she passed away 4 days after delivery. On postmortem examination, gross pathology and histopathology were both unremarkable, with the exception of liver histology that showed moderate non-specific deposition of iron in the hepatocytes and mild portal inflammation and cholestasis. Liver electron microscopy (EM) showed preservation of the cell ultrastructure but the hepatocytes were uniformly distended with small regular sized mitochondria occupying 70% of the cytoplasm. Mitochondrial granules were poorly present and the matrix was pale. Small lipid droplets were seen in some hepatocytes.

Glycogen particles were normal in structure but decreased in number. Peroxisomes were normal. Lysosomes appeared normal and were mildly increased in number. The appearance was reported to be indicative of a mitochondrial disorder. Skeletal muscle, liver and skin biopsies were collected shortly after death for mitochondrial respiratory chain enzymology. Relative to citrate synthase, liver showed 16% residual activities of complexes I and IV, while skeletal muscle had borderline low complex I (33%) and fibroblasts had deficient complex I activity (13%), with all other complexes in the normal range. This patient was included in a previously studied cohort of complex I deficiency patients (DT24[60]). She underwent full mtDNA sequencing as part of the 'MitoExome' study (P9[61]). mtDNA depletion testing of liver DNA was elevated.

P5

The patient was the first child of healthy consanguineous parents of Mauritian background with no family history of genetic disease or congenital malformations. She was born by emergency caesarean section at 36 weeks gestation due to poor cardiotocogram (CTG). Ultrasound performed two days before birth showed symmetrical IUGR and hypertrophic cardiomyopathy. Apgar scores were 2 and 6 at 1 and 5 minutes, respectively. She was mechanically ventilated at birth and transferred to a tertiary hospital where echocardiography showed a structurally normal heart but severe hypertrophic cardiomyopathy. There were no dysmorphic features, but probable bilateral cataracts were noted. Her cardiac function deteriorated despite full cardiorespiratory and inotropic support and she developed progressive metabolic acidosis with markedly elevated lactate. She died at 3 days of age. A full postmortem was not performed but biopsies of liver, heart and skeletal muscle were collected. Liver EM showed occasional small lipid droplets in the hepatocytes and mitochondria that appeared round and regular in shape, moderately increased in number, and with loose mitochondrial matrix with poorly preserved cristae. EM of cardiac and skeletal muscle showed a small number of lipid droplets and an increased number of mitochondria, which appeared swollen. These appearances were felt to be consistent with mitochondrial disease. Cardiac muscle, liver,

skeletal muscle and skin biopsies were collected 1 hour postmortem for mitochondrial respiratory chain enzymology. Relative to citrate synthase, heart showed marked deficiency of complex I (6% residual activity), while liver and skeletal muscle had more modest complex I deficiency (20% and 30%, respectively), whilst fibroblast enzymes were unremarkable. This patient was included in a previously studied cohort of complex I deficiency patients (DT98[60]). She also underwent full mtDNA sequencing (from cardiac muscle), and mtDNA depletion testing of liver DNA was normal. Splicing studies of *AGK* mRNA and Sanger sequencing were performed due to a clinical query of Sengers syndrome (MIM: 212350).

P6

The patient was the first child of a non-consanguineous couple of European (New Zealand) descent with no family history of genetic diseases or birth malformations. His mother also had two healthy children from a previous relationship. This pregnancy was complicated by a large fibroid, with frequent ultrasound monitoring as a result, which did not reveal any fetal morphological abnormalities. The male infant was delivered by emergency lower segment caesarean section at 38 weeks due to reduced fetal movement, a non-reassuring CTG and breech presentation. He was pulseless and pale at birth, requiring active resuscitation including intubation and intermittent positive-pressure ventilation (IPPV), cardiac massage and adrenaline, with the first recorded pulse at 4.5 minutes and first spontaneous breath at 20 minutes. He was noted to be hydropic with bilateral pleural effusions. He required on-going ventilation and was transferred to a tertiary neonatal intensive care unit on day 1. His birth weight (with hydrops) was 3320 gm (25^{th} - 50^{th} percentile), birth length 48 cm (25^{th} percentile), head circumference 35 cm (25^{th} - 50^{th} percentile). He was noted to have corneal opacities and some dysmorphic features (more apparent as edema resolved) with low-set, posteriorly rotated ears and short palpebral fissures. He developed hypotension after four hours, requiring ionotropic support and was noted to have cardiomegaly with marked bi-ventricular hypertrophy (right side more than left side). He was jittery from soon after birth, developed

generalized seizures from day two, which responded poorly to anti-epileptic medication, with EEG monitoring showing depressed electrical activity with burst-suppression. MRI showed T1 hypointensity and T2-hyperintensity of the cerebral and cerebellar white matter, striking swelling of the cerebral white matter, and subtle T2 signal abnormality in the basal ganglia with dots of T1 hyperintensity, indicative of hemorrhage or calcification. He developed lactic acidosis which progressively worsened (peak 13 mmol/L). A “mitochondrial cocktail” of biotin, thiamine, riboflavin, carnitine and co-enzyme Q10 was trialed with no response. Urine organic acid analysis showed a mixed lactic and keto-acidosis with TCA metabolites, including 3-methylglutaconic acid, consistent with a respiratory chain disorder. On day three his respiratory and cardiovascular condition deteriorated, he developed asystole while still on the ventilator and passed away at age 64 hours. Multiple additional investigations were performed to rule out other causes of non-immune hydrops, corneal clouding and cardiomyopathy, all yielding normal results. These included white cell enzyme analysis, antenatal TORCH infection testing, cholesterol and 7-dehydrocholesterol, urine mucopolysaccharides, acyl-carnitine profile and testing for peroxisomal disorders. Postmortem examination confirmed multi-system disease including: bi-ventricular hypertrophic cardiomyopathy; ophthalmological abnormalities including microphthalmia and corneal opacities; CNS abnormalities including ill-defined basal ganglia and thalami; cerebral white matter necrosis, with rarefaction and gliosis of peri-ventricular white matter; perivascular mineralized bodies with the appearance of psammoma bodies principally in basal ganglia and thalamus; hepatic steatosis and early bridging fibrosis. Postmortem heart, skeletal muscle and liver samples were sent for respiratory chain analysis, and a fibroblast cell line was established. Relative to citrate synthase, heart and liver showed marked deficiency of complex I (3% and 4% residual activity, respectively) as well as low complex IV (20% and 14% residual activity, respectively) while skeletal muscle had low activities of all enzymes with only complex I clearly deficient relative to citrate synthase (13%). Subsequent quantitative PCR analysis from liver DNA excluded mtDNA depletion and single or multiple mtDNA deletions, while muscle mtDNA was decreased (possibly due to poor muscle development). Full

mtDNA sequencing did not reveal any pathogenic mutations. This patient was included in a previously studied cohort of complex I deficiency patients (DT86[60]).

P7

This male infant was born at almost 37 weeks gestation by elective caesarean section during labor for breech presentation. Apgars were 3, 6 and 9 at 1, 5 and 10 minutes, respectively. He was the second child to unrelated parents of European (Australian) descent whose first child died at 6 days of age, with what was described as hypoxic ischemic encephalopathy but for which no obstetric cause was found. At birth, this patient was noted to have generalized edema and chest X-ray showed a grossly enlarged heart. His birth weight was 2460 gm (< 10th percentile), length 43 cm (< 3rd percentile) and head circumference 34.5 cm (50th - 90th percentile). Corneal opacities were observed. Cardiac echocardiogram demonstrated persistent pulmonary hypertension and ventricular hypertrophy with reduced systolic function. He developed seizures in the first hours after birth. Capillary lactate was 4.0 mmol/L (NR 0.6-2.4) and CSF lactate 4.5 mmol/L (1.2-2.1). Urine organic acids on day 1 showed traces of fumaric and 3-methylglutaric acids. Repeat testing on day 2 showed traces of fumaric, 3-methylgutaric and 3-methylglutaconic acids. Amino acids were normal in plasma with slightly increased taurine in urine. A skeletal muscle biopsy was taken for mitochondrial respiratory chain enzymology, following which he deteriorated and died. Samples of heart, liver, further skeletal muscle and skin samples were collected <3 hours postmortem. Relative to citrate synthase, heart and liver showed marked deficiency of complex I (6% residual activity in both) with complex IV also somewhat low in liver (31%). In skeletal muscle, complex I was at the lower end of the normal range (48%). At postmortem, he had evidence of peripheral and cerebral edema. There were small pleural and pericardial effusions and a small amount of ascitic fluid was noted. The heart was enlarged with ventricular hypertrophy. On histologic examination, there was subendocardial fibrosis and prominent glycogenic vacuolation of the adjacent myocardial cells with no other glycogenic vacuolation or features of glycogen storage disorder. Heart EM was not performed. There

appeared to be softening of the right caudate nucleus and right fronto-parietal region in the subcortical white matter on macroscopic brain examination, but no abnormalities were found on microscopic examination. Purkinje cells in the cerebellum were reported to have slightly vacuolated nuclei but no other abnormalities. This patient was included in a previously studied cohort of complex I deficiency patients (DT106[60]). mtDNA deletion studies in liver and skeletal muscle were normal.

P8

The patient was one of dizygous twins, the first pregnancy of healthy non-consanguineous parents with no family history of genetic diseases or congenital abnormalities. *In utero* ultrasonography had suggested possible tachyarrhythmia but follow up scans were normal. He was delivered at 38 weeks pregnancy by vaginal breech delivery with birth weight 2.5 kg (3^{rd} - 10^{th} percentile). Apgars were 4 and 6 at 1 and 5 minutes, respectively. His twin sister was healthy. He developed paroxysmal atrial tachycardia associated with cardiomegaly and cardiac failure on the first day of life. Echocardiography showed asymmetric hypertrophic cardiomyopathy predominantly affecting the right ventricle. He was subsequently noted to be hypotonic and had hepatomegaly. He had marked metabolic acidosis with raised CSF and blood lactate. A cranial ultrasound showed Grade III intraventricular hemorrhages, patchy echogenicity in the basal ganglia and small cystic lesions in the region of the right head of the caudate. He was noted to have a prominent forehead and relatively small jaw. Despite full cardiorespiratory and inotropic support, he developed progressive left ventricular dilation, cardiac failure, peripheral edema and ascites, and died at 8 days of age. At autopsy, the heart was structurally normal but markedly enlarged, with mild endocardial fibroelastosis of the right ventricle. The liver showed marked fatty changes and on EM, mitochondria appeared prominent and increased in number but structurally normal, although they often had a pale matrix. The brain showed evidence of focal damage in the form of gliosis, neuronal loss and cystic change, and there was marked spotty calcification in the basal ganglia. The dentate nuclei

showed considerable shrinkage of neurons. Cardiac muscle, liver, skeletal muscle and skin biopsies were collected 2 hours postmortem for mitochondrial respiratory chain enzymology. Relative to citrate synthase, heart and liver showed marked deficiency of complex I (5% and 3% residual activity, respectively) with complex IV also somewhat low in liver (25%). Respiratory chain enzymes in skeletal muscle and fibroblasts were unremarkable. Activities in liver showed 4% complex I activity (compared to control mean and relative to citrate synthase) and a borderline decrease in complex IV activity (25% residual activity). His fibroblast and muscle enzymes were all within normal range. This patient was included in a previously studied cohort of complex I deficiency patients (DT93[60]). mtDNA depletion testing of liver crud DNA was normal.

P9

The female infant was the first child of a non-consanguineous couple, with the patient's 27-year-old mother having normal/ low risk results for her early pregnancy, routine first trimester and routine second trimester investigations. CMV serology was not performed. She presented at 26 weeks with suspected IUGR. She had decreased fetal movements at 34 weeks' gestation. Ultrasound scans confirmed IUGR with severe oligohydramnios and she was delivered by emergency caesarean section. The infant was judged to be in poor condition at delivery and required bag and mask resuscitation, intermittent CPAP and incubator oxygen for a few hours before weaning to room air. Her Apgar scores were 4 and 7 at 1 and 5 minutes, respectively. Her birth weight was 1761 gm, and her head circumference 30 cm (both < 10^{th} percentile); her length was 45 cm (10^{th} - 50^{th} percentile). She subsequently had multiple cyanotic episodes not associated with apnea. Echocardiography demonstrated poor left ventricular function, ventricular hypertrophy and endocardial fibroelastosis. She was intubated for mechanical ventilation from 36 hours of age (peak ventilation 22/5, Rate 50/min, 85% O_2) for cardiac failure. She was commenced on antibiotics for suspected sepsis. Her bacterial cultures were negative and her CRP peaked at 11.6 on day 3. Placental tissue cultured *Klebsiella pneumoniae*. Gancyclovir was added to the regimen when CMV PCR was positive for CMV.

Investigations for other viruses were negative. Her cranial ultrasound scan on day 1 showed sub-ependymal cysts and lenticular striate artery echogenicity, consistent with congenital CMV infection. She then developed systemic hypotension and cardiac failure, requiring multiple inotropic agents including dopamine, dobutamine, milrinone and adrenaline infusion. Her perfusion remained poor with worsening metabolic acidosis. She was treated with volume expansion, red cell transfusions for anemia, albumin transfusions for hypoalbuminemia, fresh frozen plasma for coagulopathy and sodium bicarbonate for acidosis. However, the acidosis was unresponsive to correction. She had a cord blood lactate of 5.3 mmol/L, a serum arterial blood lactate of 9.4 mmol/L at 11 hours of age, a CSF lactate of 13.5 mmol/L on day 1 of life and a peak arterial blood lactate of 25 on day 5 of life. Her blood ammonia was mildly elevated at 74 μmol/L on day 2. GGT was elevated (301 U/L) but alanine aminotransferase (ALT) was not indicative of hepatitis. The attending clinicians thought that the clinical picture was more likely to have a mitochondrial rather than an infective cause. She developed acute renal failure with oliguria on day 3 that was unresponsive to frusemide treatment. The patient eventually had bradycardia and cardiac arrest on day 6 of life while on maximal inotropic support and could not be resuscitated. Her parents agreed to postmortem tissue sampling of her myocardium, skeletal muscle, liver and skin for mitochondrial studies and consented to a formal postmortem examination. Histopathology of the perimortem biopsies showed normal appearance of heart and skeletal muscle with hemosiderosis as the only liver tissue finding. EM showed moderate fatty change in hepatocytes with moderately swollen mitochondria thought to be secondary to autolysis. The ultrastructure of the heart and skeletal muscle was poorly preserved and could not be assessed for features of metabolic disorders. Clinical postmortem examination recorded a diffusely enlarged heart with thickening of the walls of both ventricles and of the intraventricular septum. Myocardial histology showed clear to pale cytoplasm with peripheral eosinophilic condensation, pyknotic nuclei and scattered apoptotic bodies. Liver pathology showed firm and pale tan/yellow parenchyma. Histopathology showed definite mitochondrial pathology with enlarged hepatocytes containing pale vacuolated foamy cytoplasm. There was marked intrahepatic iron accumulation.

Brain histology showed evidence of hypoxia/ ischemia. There was no postmortem evidence of myocarditis and none of the organ systems studied showed evidence of viral pathology. Cardiac muscle, liver, skeletal muscle and skin biopsies were collected shortly after death for mitochondrial respiratory chain enzymology. Relative to citrate synthase, heart and liver showed marked deficiency of complex I (1% and 10% residual activity, respectively) with complex IV and complex III also low in liver (13% and 19%, respectively). In skeletal muscle, complex I was borderline low (35%) while fibroblast enzymes were unremarkable. This patient was included in a previously studied cohort of complex I deficiency patients (DT101[60]).

P10

This male infant was born weighing 3.1 kg (10^{th} - 50^{th} percentile) at 40 weeks gestation; the second child of non-consanguineous Japanese parents. There was no family history of neuromuscular disease. At birth, the patient presented with respiratory distress and hypotonia with Apgar scores of 3 and 4 at 1 and 5 minutes, respectively, and needed intubation. Physical examination revealed cloudy corneas. Echocardiography at birth showed diffuse hypertrophy in both ventricles with left ventricular end-diastolic posterior wall thickness (LVPWd) of 4.2 mm (Z-score: 2.1), intraventricular septum thickness at end-diastole (IVSd) of 10.4 mm (Z-score: 5.0) and normal left ventricular ejection fraction. Brain MRI revealed a diffuse cerebral white matter abnormality with low signal on T1 weighted image and high signal on T2 weighed image. Automated auditory brain stem response showed bilateral hearing loss. He had elevated lactate (9.9 mmol/L) and an elevated lactate/pyruvate ratio (27.8) at 54 days after birth. The patient died at 76 days after birth due to progressive respiratory failure and heart failure. Relative to citrate synthase, heart showed marked deficiency of complex I (5% residual activity) and borderline low complex IV activity (36%) while complex I was at the lower end of the normal range in liver and skeletal muscle (41% and 45%, respectively) and unremarkable in fibroblasts.

P11

The male patient was born weighing 3.0 kg (50^{th} - 75^{th} percentile) at 37 weeks gestation from non-consanguineous Japanese parents. At birth, the patient required intubation due to respiratory distress and meconium staining with Apgar scores of 2 and 10 at 1 and 5 minutes, respectively. His cranial ultrasound revealed bilateral bright thalami. Echocardiography at birth showed left ventricular hypertrophy with LVPWd of 4.1 mm (Z-score: 2.0), IVSd of 7.9 mm (Z-score: 3.7) and normal left ventricular ejection fraction. Although he underwent successful extubation at 5 days, he needed re-intubation at 10 days after birth due to a severe apnea attack. Echocardiography at 10 days revealed pericardial effusion. At 23 days after birth, the patient experienced cardiac tamponade which required pericardial drainage. He had elevated levels of lactate in blood and CSF (both 9.9 mmol/L) with raised lactate/pyruvate ratios (27.5 and 29.1, respectively). The patient died at 32 days after birth due to heart failure. Relative to citrate synthase, heart showed marked deficiency of complex I (5% residual activity) while complex I was borderline low in liver (29%). Skeletal muscle had low activities of all enzymes with complex I in the lower part of the normal range relative to citrate synthase (57%) and unremarkable in fibroblasts.

P12

This female patient was diagnosed with IUGR and born by emergency caesarean section at 36 weeks gestation because of non-reassuring fetal status with Apgar scores of 4 and 6 at 1 and 5 minutes (respectively) and weighed 1.7 kg (< 3^{rd} percentile). The patient required intubation due to neonatal asphyxia. Physical examination revealed cloudy corneas, microphthalmia, abnormal iris, and arthrogryposis. Her brain CT showed mild calcification in the lenticular nucleus. At day 2 after birth, her blood lactate level was elevated at 12.6 mmol/L with an elevated lactate/pyruvate ratio of 36.0. At day 19 after birth, she developed heart failure. Her echocardiography showed mild diffuse hypertrophy and enlarged left ventricle with LVPWd of 2.8 mm (Z-score: 0.5), IVSd of 4.8 mm (Z-score: 1.7), left ventricular end-diastole diameter of 18.7mm (Z-score: 1.9), decreased left ventricle

ejection fraction (49%) and pericardial effusion. The patient died at 27 days after birth due to worsening heart failure. Respiratory chain enzymology in skin fibroblasts showed no significant decrease in any complex activity.

P13

The female patient was born weighing 2.9 kg (10th percentile) at 40 weeks gestation from non-consanguineous Japanese parents. At birth, the patient presented with respiratory distress and hypotonia with Apgar scores of 6 and 7 at 1 and 5 minutes). Echocardiography at three days after birth showed diffuse hypertrophy in both ventricles with LVPWd of 4.1 mm (Z-score: 2.0), IVSd of 5.1 mm (Z-score: 1.7), decreased left ventricular ejection fraction (46%), and pericardial effusion. She had an elevated blood lactate (12.3 mmol/L) with an elevated lactate/pyruvate ratio of 49.2. Brain CT showed diffuse cerebral white matter hypodensity and swelling, as well as low density in the basal ganglia and thalamus. Despite the correction of progressive lactic acidosis and respiratory support for progressive respiratory failure, the patient died at 10 days after birth due to progressive heart failure. Relative to citrate synthase, heart and liver showed marked deficiency of complex I (2% and 11% residual activity, respectively) with complex IV borderline low in heart (29%) and complexes III and IV borderline low in liver (26% and 37%, respectively).

P14

This was the third child of unrelated parents of European (Australian) background. There were two older healthy siblings. The pregnancy was complicated by reduced fetal movements, prompting induction of labor at 37 weeks gestation. CTG monitoring during labor was normal. Apgar scores were 5 and 8 at 1 and 5 minutes, respectively. Birth weight was 3200 gm (63rd percentile). There was respiratory distress from birth associated with worsening metabolic acidosis that escalated, prompting elective intubation and transfer to a tertiary unit. He was noted to have bilateral corneal opacities and congenital cataracts (the latter detected by ocular ultrasound) with no evidence of glaucoma. He had a depressed level of alertness with few spontaneous movements. He developed

seizures that were treated with phenobarbitone, and the EEG showed a burst-suppression pattern. He had suspected non-immune hydrops, with edema of the head, face and limbs, with external edema continuing to worsen. He also had cardiomegaly on chest X-ray, but had no clinical features of congestive cardiac failure. His clinical condition continued to deteriorate, with bradycardia then cardiac arrest whilst being ventilated. Resuscitation was not initiated and he died at 3 days of age. His initial blood lactate was 2.3 mmol/L (NR 0.7 – 2.0), which worsened, with most subsequent levels being between 5 to 15 mmol/L. Urine amino acid analysis showed a slight increase in pipecolic acid, and organic acids showed a gross increase in lactate, and slight increases in fumarate and 3-methylglutaconic acid. Tyrosine metabolites were also seen. Normal investigations included plasma acylcarnitines, serum transferrin isoforms, serum 7-dehydrocholesterol, plasma very long chain fatty acids, and a comparative genomic hybridization array (Agilent SurePrint G3 array – mean effective resolution 0.2 Mb). Skeletal muscle, liver and skin samples were collected within two hours of death. Relative to citrate synthase, liver showed marked deficiency of complex I (2% residual activity) and low activity of complex IV (24%), while skeletal muscle enzymes were unremarkable. Full mtDNA sequencing performed using targeted mtDNA-seq[81] was normal. A head ultrasound showed bilateral subependymal hemorrhages and echogenic thalami, suggestive of an ischemic process. In addition, there was a probable calcific density in the left parietal lobe. At autopsy, hydrops with ascites, pleural effusions and subcutaneous edema were noted. He was not dysmorphic. The heart weight was 35.7 g (NR 17.0 +/- 3.8), with right and left ventricles of normal morphology but dilated. Gross brain morphology appeared normal but there was widespread gliosis and microglial activation with some neuronal loss. Changes in the basal ganglia were more severe dorsally than ventral. The liver was enlarged. The kidneys showed fetal lobulation but were otherwise normal structurally and histologically. Histological examination of skeletal muscle was unremarkable, whilst Perls staining of the liver revealed hepatic siderosis and there was also microvesicular steatosis. There was a diffuse abnormality of lung growth with arrested alveolar development consistent with congenital alveolar dysplasia.

P15

The male infant was the second child of non-consanguineous European (Australian) parents with no family history of genetic diseases or birth malformations. Early fetal scans revealed IUGR, with a scan at 31 weeks gestation suggestive of cardiac hypertrophy. At 36 weeks gestation severe hydrops was noted, with bilateral pleural effusions, but no ascites or pericardial effusion. At this time hypertrophic cardiomyopathy with mild tricuspid incompetence was identified. He also had a 2-vessel umbilical cord and hypospadias was suspected. Fetal death *in utero* occurred at 36 + 6 weeks gestation. Autopsy weight was 2240 gm (10^{th} percentile), length was 44.3 cm ($<10^{th}$ percentile), consistent with IUGR, and head circumference was 28.0 cm (NR 30.8 +/- 1.9). There was extensive skin slippage, consistent with severe subcutaneous edema. He had no dysmorphic facial features, and no corneal clouding or cataracts were observed. Genitalia were normal with no evidence of hypospadias. Bilateral pleural effusions and a pericardial effusion were also noted. The heart weight was 19.5 g (NR 14.5 +/- 3.3). The right (free wall 5-6 mm; normal 3.1 mm) and left (free wall 10 mm; normal 3.8 mm) ventricles were hypertrophic, but with normal cardiac anatomy. Gross brain morphology appeared normal but there was gliosis and microglial activation with some neuronal loss in the brainstem, cerebellum, thalamus and basal ganglia, more severe dorsally than ventral. Histological examination of liver, kidneys and skeletal muscle were unremarkable, whilst in the heart the endocardium was thickened with fibroelastosis, most marked in the left ventricle. There was also evidence of early pulmonary hypoplasia. Meconium peritonitis was also noted.

P16

This male infant was delivered by spontaneous vaginal birth at term plus 11 days, with a birth weight of 3.5 kg (50^{th} percentile) and Apgar scores of 3, 4 and 6 at 1, 5 and 10 minutes, respectively. The pregnancy and family history were unremarkable, and the parents were of non-consanguineous European (Australian) descent. The CTG trace during labor showed reduced variability and meconium was noted at delivery. The cord arterial blood pH was 7.34. Seizures were first noted at

15 minutes of age and continued throughout the admission although the EEG did not provide support for a specific seizure-type. The MRI showed mild signal abnormality and swelling of the cerebral white matter with highly increased lactate signal in MRS. The findings were considered similar to hypoxic ischemic encephalopathy. Hypotension was noted early and required treatment with dopamine, dobutamine and adrenaline. Anuria and steadily worsening renal function were also present and there was a mild coagulopathy. The initial echocardiogram demonstrated severe biventricular cardiac dysfunction with mild ventricular hypertrophy; however, a repeat echocardiogram three days later showed considerably improved function. Although an inherited cardiomyopathy was thought possible, the initial dysfunction was considered likely secondary to the metabolic acidosis. Corneal clouding was also noted. Lactic acidosis (lactate 6.7 mmol/L; NR <2.0) was present on arrival at the tertiary care center and steadily worsened until lactate was in the range 40–50 mmol/L before death on day 7. The urine metabolic screen showed increased 3-methyglutaconate (170 μmol/mmol creatinine; NR <15), 3-methylglutarate, fumarate and lactate, and a mild increase in S-sulfocysteine. The plasma amino acids showed increased alanine and decreased cystine. The clinical and biochemical features suggested there might be an underlying mitochondrial disorder. Skeletal muscle respiratory chain enzymology was unremarkable and full mtDNA sequencing was normal. Fibroblast pyruvate dehydrogenase enzymology and cardiolipin assay were normal. ATP synthase (complex V) was assessed by SDS-PAGE western blot of fibroblast protein and showed no evidence for a decrease in ATP synthase subunit alpha protein. The muscle light microscopy initially showed “prominent mitochondria” suggesting a possible mitochondrial cytopathy. However, EM subsequently showed abundant membrane-bound structures (autophagosomes without basal lamina) consistent with an autophagic vacuolar myopathy. It was thought the widespread positive staining seen on Gomori Trichrome stain was probably due to autophagosomes and not prominent mitochondria as originally reported. Glycogen and lipid were not increased. EM of cultured skin fibroblasts showed a moderate increase in the number of “autophagosomes” within some fibroblasts but the finding was not widespread. Additional normal

investigations included plasma acylcarnitines, plasma ammonium, plasma iron studies, bloodspot α-glucosidase, urine mucopolysaccharides and oligosaccharides, fibroblast lysosomal enzyme screen, and *LAMP2* sequencing. The chromosomes showed a normal male karyotype. Placental examination was unremarkable apart from significant meconium staining of the membranes. A postmortem examination was declined.

Supplemental Table 2. Paired alignment of the *ATAD3A* and *ATAD3C* genomic DNA sequence surrounding the duplications, related to **Figure 2**.

GRCh37/hg19 regions chr1:g.1,390,475-1,395,618 (*ATAD3C*) and chr1:g.1,458,523-1,462,918 (*ATAD3A*) were aligned using EMBOSS Needle (https://www.ebi.ac.uk/Tools/psa/emboss_needle/). Lines indicate identical bases, and areas corresponding to exons (blue) and exon boundaries (light blue) within *ATAD3C* and *ATAD3A* are annotated. The different duplication groups (*a-d*) along with the individual patients within these groups and their corresponding breakpoint genomic coordinates are indicated. Red bases identify the 5' *ATAD3C* and 3' *ATAD3A* duplication breakpoints.


ATAD3C
CCTGCCTGCAGGTGTCTGGGGGGCTCAGCTGCCTGGGGAATGGACCCCCCTTAGGCCTTTGCCCACCCTCGTGTAGGCTCAGGGTGCTGGTGTGGGCAGCAGCGCCTCCCATCTTCCAGGCGGGGGA
ATAD3A
CCTGCCTGCAGGTGTCTGGGGGGCTCAGCTGCCTGGGGAATGGACCCCCCTTAGGCCTTTGCCCACCCTCGTGTAGGCTCAGGGTGCTGGTGTGGGCAGCAGCGCCTCCCATCTTCCAGGCGGGGGA
Duplication group a
P12
1:1391576
ATAD3C
CGTCTCCTGTCTGGCAGGCTGTGGCTTCCAGGCAGGGACGCTGGGCAGAGCCTCCACACTCCGGGTGGAGTGTGCAGGCTTTGCAGAGGCGGAGGGAACATCTGTTCTGTCTCCCCTCACTCTTCTT
ATAD3A
CGTCTCCTGTCTGGCAGGCTGTGGCTTCCAGGCAGGGACGCTGGGCAGAGCCTCCACACTCCGGGTGGAGTGTGCAGGCTTTGCAGAGGCGGAGGGAACATCTGCTCTGTCTCCCCTCACTCTTCCT
1:1459623
Exon 7
ATAD3C
GTCCAGAAACTCGCCCTGCACTCAGGCATGGACTACGCCATCATGACAGGCGGGGACGTGGCCCCCATGGGGCGGGAAGGCGTGACCGCCATGCACAAGCTCTTTGACTGGGCCAATACCAGCCGGC
ATAD3A
GTCCAGAAACTCGCCCTGCACTCAGGCATGGACTACGCCATCATGACAGGCGGGGACGTGGCCCCCATGGGGCGGGAAGGCGTGACCGCCATGCACAAGCTCTTTGACTGGGCCAATACCAGCCGGC
Exon 11
ATAD3C
GCGGGTGAGACGTCCCCACAGCATGCACCAGGCCCTTGGCTGCGGCCCAGCAGGCTGCCTTCTGGGAAGGGGGTCCAGGTGTCTCTTGGGGACCCTGTCTTTCTGCAGCTCTGTCCTTGTGGCCACG
ATAD3A
GCGGGTGAGACGTCCCCACAGCATGCACCAGGCCCTTGGCTGCGGCCCAGCAGGCTGCCTTCTGGGAAGGGGGTCCAGGTGTCTCTTGGGGACCCTGTCTTTCTGCAGCTCTGTCCTTGTGGCCACG
ATAD3C
CAGGAGGCCCAGTGGAGGGTCCCTCGGAGGGAAAGTCCCCTGAGTGTGGACCCTGGTGGACACGAGGCCCCCAGCGTGTGGAGGCTGCCAGTGGGATACTTGGCTCAGGGCAGAAGGGAGGTGGGTG
ATAD3A
CAGGAGGCCCAGTGGAGGGTCCCTCGGAGGGAAAGTCCCCTGAGTGTGGACCCTGGTGGACACGAGGCCCCCAGCGTGTGGAGGCTGCCAGTGGGATACTTGGCTCAGGGCAGAAGGGAGGTGGGTG
Duplication group b
P2a/b, P4, P6, P8, P9, P10, P11, P13-P16
1:1391996
ATAD3C
GGTGCAGGGGGAGAGGGGTCTTCACAGCTGCAGGGGAGGCTCCTCCACAGCCGCCCTCCCCCCAACACGCCTGCAGGTGGGCGTGGGCACTGGTTGCCTTTTCTAGAACCATTTGAAAGTTAGCTGA
ATAD3A
GGTGCAGGGGGAGAGGAGTCTTCACAGCTGCAGGGGAGGCTCCTCCACAGCCGCCCTCCCCCCAACACGCCTGCAGGTGGGCGTGGGCACTGGTTGCCTTTTCTAGAACCATTTGAAAGTTAGCTGA
1:1460043
ATAD3C
AGACAGCATGGCACACTCCCTTCAATAGGTCCCACAGTGACCCCGCGCAGGGCACAGCCCGGGCACCCTTGTGGCCTCGGCTGTCCTCGTTGGAACCACGATGCTCATGGTTGGCACCCTCCCCTCT
ATAD3A
AGACAGCATGGCACACTCCCTTCAATAGGTCCCACAGTGACCCCGCGCAGGGCACAGCCCGGGCACCCTTGTGGCCTCGGCTGTCCTCGTTGGAACCACGATGCTCATGGTTGGCACCCTCCCCTCT

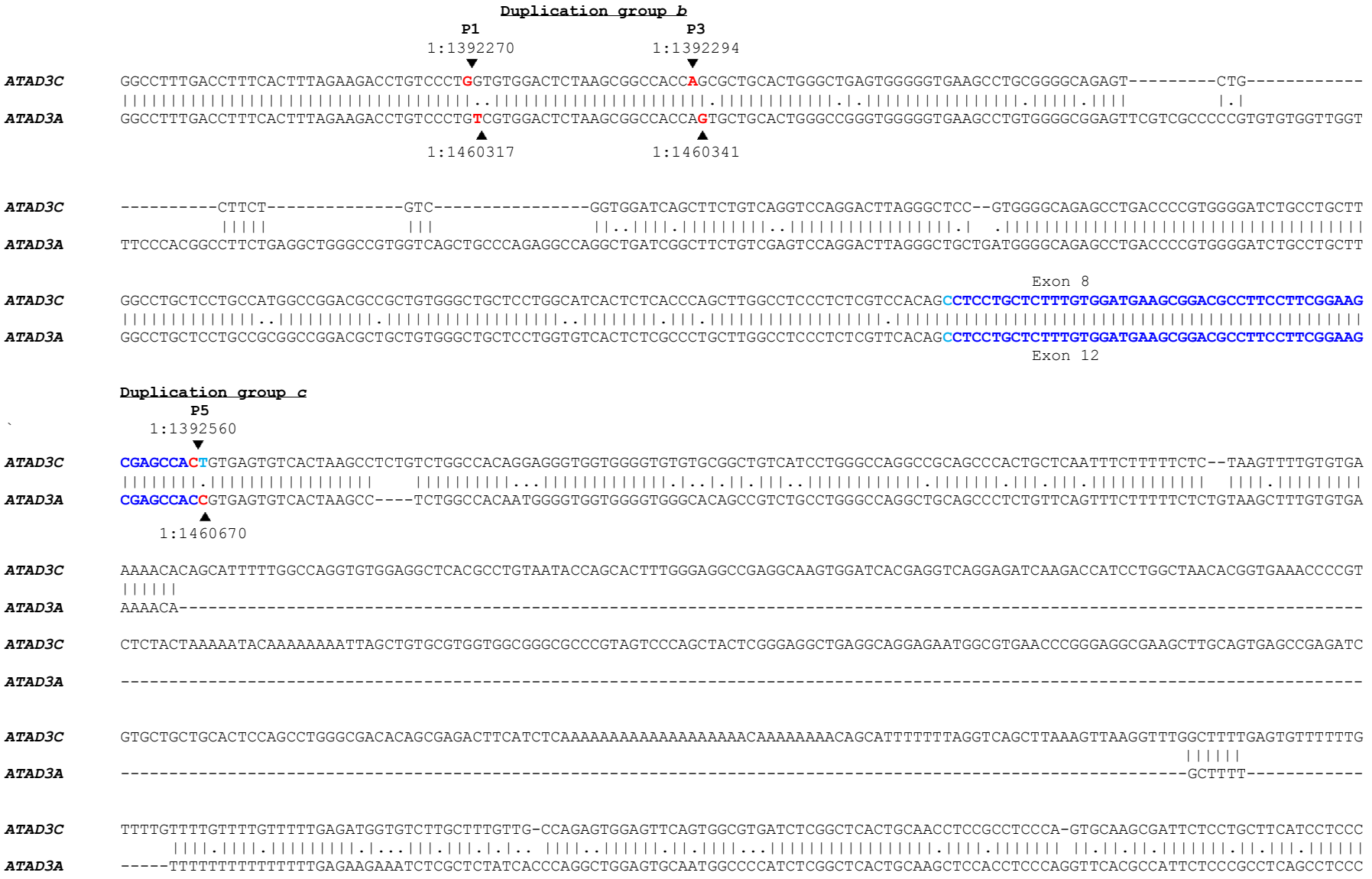
Duplication group b
P1
P3
1:1392270
1:1392294
ATAD3C
ATAD3A
1:1460317
1:1460341
Exon 8
Exon 12
Duplication group c
P5
1:1392560
1:1460670

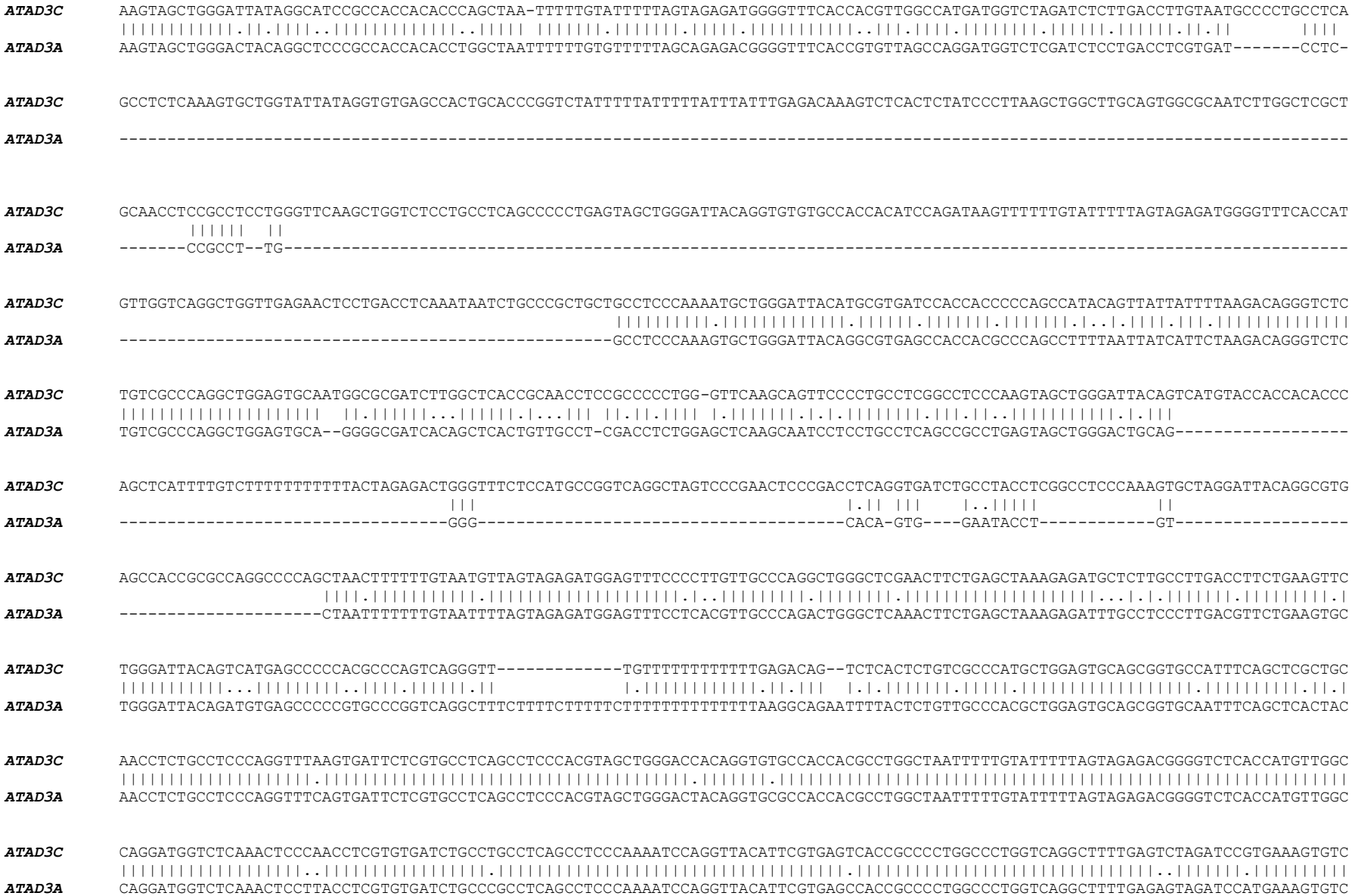
ATAD3C
AAGTAGCTGGGATTATAGGCATCCGCCACCACACCCAGCTAA-TTTTTGTATTTTTAGTAGAGATGGGGTTTCACCACGTTGGCCATGATGGTCTAGATCTCTTGACCTTGTAATGCCCCTGCCTCA
ATAD3A
AAGTAGCTGGGACTACAGGCTCCCGCCACCACACCTGGCTAATTTTTTGTGTTTTTAGCAGAGACGGGGTTTCACCGTGTTAGCCAGGATGGTCTCGATCTCCTGACCTCGTGAT-------CCTC-
ATAD3C
GCCTCTCAAAGTGCTGGTATTATAGGTGTGAGCCACTGCACCCGGTCTATTTTTATTTTTATTTATTTGAGACAAAGTCTCACTCTATCCCTTAAGCTGGCTTGCAGTGGCGCAATCTTGGCTCGCT
ATAD3A
ATAD3C
GCAACCTCCGCCTCCTGGGTTCAAGCTGGTCTCCTGCCTCAGCCCCCTGAGTAGCTGGGATTACAGGTGTGTGCCACCACATCCAGATAAGTTTTTTGTATTTTTAGTAGAGATGGGGTTTCACCAT
ATAD3A
-------CCGCCT--TG----------
ATAD3C
GTTGGTCAGGCTGGTTGAGAACTCCTGACCTCAAATAATCTGCCCGCTGCTGCCTCCCAAAATGCTGGGATTACATGCGTGATCCACCACCCCCAGCCATACAGTTATTATTTTAAGACAGGGTCTC
ATAD3A
----------GCCTCCCAAAGTGCTGGGATTACAGGCGTGAGCCACCACGCCCAGCCTTTTAATTATCATTCTAAGACAGGGTCTC
ATAD3C
TGTCGCCCAGGCTGGAGTGCAATGGCGCGATCTTGGCTCACCGCAACCTCCGCCCCCTGG-GTTCAAGCAGTTCCCCTGCCTCGGCCTCCCAAGTAGCTGGGATTACAGTCATGTACCACCACACCC
ATAD3A
TGTCGCCCAGGCTGGAGTGCA--GGGGCGATCACAGCTCACTGTTGCCT-CGACCTCTGGAGCTCAAGCAATCCTCCTGCCTCAGCCGCCTGAGTAGCTGGGACTGCAG----------
ATAD3C
AGCTCATTTTGTCTTTTTTTTTTTACTAGAGACTGGGTTTCTCCATGCCGGTCAGGCTAGTCCCGAACTCCCGACCTCAGGTGATCTGCCTACCTCGGCCTCCCAAAGTGCTAGGATTACAGGCGTG
ATAD3A
----------GGG----------CACA-GTG----GAATACCT----------GT----------
ATAD3C
AGCCACCGCGCCAGGCCCCAGCTAACTTTTTTGTAATGTTAGTAGAGATGGAGTTTCCCCTTGTTGCCCAGGCTGGGCTCGAACTTCTGAGCTAAAGAGATGCTCTTGCCTTGACCTTCTGAAGTTC
ATAD3A
----------CTAATTTTTTTGTAATTTTAGTAGAGATGGAGTTTCCTCACGTTGCCCAGACTGGGCTCAAACTTCTGAGCTAAAGAGATTTGCCTCCCTTGACGTTCTGAAGTGC
ATAD3C
TGGGATTACAGTCATGAGCCCCCACGCCCAGTCAGGGTT----------TGTTTTTTTTTTTTGAGACAG--TCTCACTCTGTCGCCCATGCTGGAGTGCAGCGGTGCCATTTCAGCTCGCTGC
ATAD3A
TGGGATTACAGATGTGAGCCCCCGTGCCCGGTCAGGCTTTCTTTTCTTTTTCTTTTTTTTTTTTTTTAAGGCAGAATTTTACTCTGTTGCCCACGCTGGAGTGCAGCGGTGCAATTTCAGCTCACTAC
ATAD3C
AACCTCTGCCTCCCAGGTTTAAGTGATTCTCGTGCCTCAGCCTCCCACGTAGCTGGGACCACAGGTGTGCCACCACGCCTGGCTAATTTTTGTATTTTTAGTAGAGACGGGGTCTCACCATGTTGGC
ATAD3A
AACCTCTGCCTCCCAGGTTTCAGTGATTCTCGTGCCTCAGCCTCCCACGTAGCTGGGACTACAGGTGCGCCACCACGCCTGGCTAATTTTTGTATTTTTAGTAGAGACGGGGTCTCACCATGTTGGC
ATAD3C
CAGGATGGTCTCAAACTCCCAACCTCGTGTGATCTGCCTGCCTCAGCCTCCCAAAATCCAGGTTACATTCGTGAGTCACCGCCCCTGGCCCTGGTCAGGCTTTTGAGTCTAGATCCGTGAAAGTGTC
ATAD3A
CAGGATGGTCTCAAACTCCTTACCTCGTGTGATCTGCCCGCCTCAGCCTCCCAAAATCCAGGTTACATTCGTGAGCCACCGCCCCTGGCCCTGGTCAGGCTTTTGAGAGTAGATCCATGAAAGTGTC

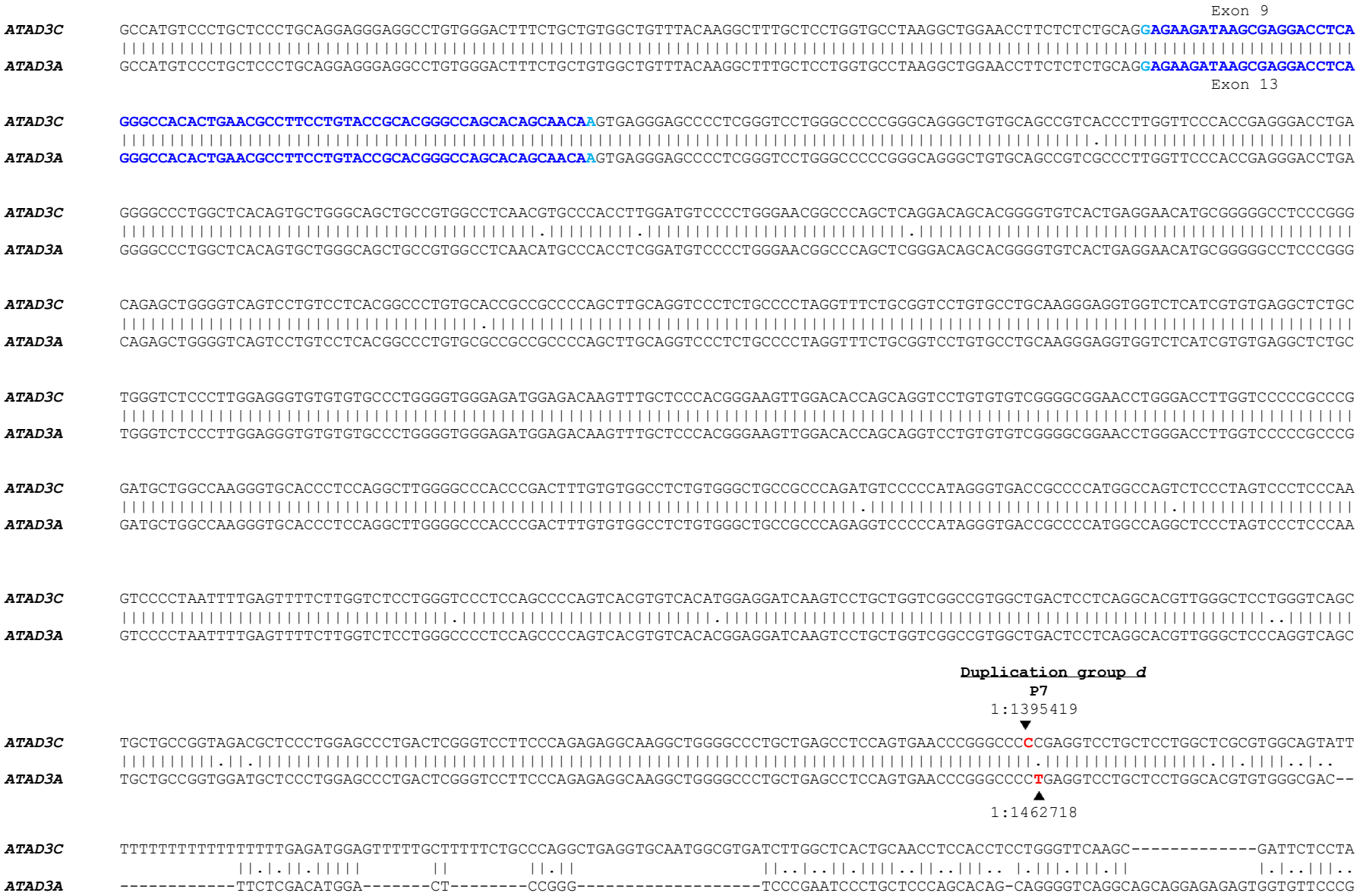
Exon 9
ATAD3C
GCCATGTCCCTGCTCCCTGCAGGAGGGAGGCCTGTGGGACTTTCTGCTGTGGCTGTTTACAAGGCTTTGCTCCTGGTGCCTAAGGCTGGAACCTTCTCTCTGCAGGAGAAGATAAGCGAGGACCTCA
ATAD3A
GCCATGTCCCTGCTCCCTGCAGGAGGGAGGCCTGTGGGACTTTCTGCTGTGGCTGTTTACAAGGCTTTGCTCCTGGTGCCTAAGGCTGGAACCTTCTCTCTGCAGGAGAAGATAAGCGAGGACCTCA
Exon 13
ATAD3C
GGGCCACACTGAACGCCTTCCTGTACCGCACGGGCCAGCACAGCAACAAGTGAGGGAGCCCCTCGGGTCCTGGGCCCCCGGGCAGGGCTGTGCAGCCGTCACCCTTGGTTCCCACCGAGGGACCTGA
ATAD3A
GGGCCACACTGAACGCCTTCCTGTACCGCACGGGCCAGCACAGCAACAAGTGAGGGAGCCCCTCGGGTCCTGGGCCCCCGGGCAGGGCTGTGCAGCCGTCGCCCTTGGTTCCCACCGAGGGACCTGA
ATAD3C
GGGGCCCTGGCTCACAGTGCTGGGCAGCTGCCGTGGCCTCAACGTGCCCACCTTGGATGTCCCCTGGGAACGGCCCAGCTCAGGACAGCACGGGGTGTCACTGAGGAACATGCGGGGGCCTCCCGGG
ATAD3A
GGGGCCCTGGCTCACAGTGCTGGGCAGCTGCCGTGGCCTCAACATGCCCACCTCGGATGTCCCCTGGGAACGGCCCAGCTCGGGACAGCACGGGGTGTCACTGAGGAACATGCGGGGGCCTCCCGGG
ATAD3C
CAGAGCTGGGGTCAGTCCTGTCCTCACGGCCCTGTGCACCGCCGCCCCAGCTTGCAGGTCCCTCTGCCCCTAGGTTTCTGCGGTCCTGTGCCTGCAAGGGAGGTGGTCTCATCGTGTGAGGCTCTGC
ATAD3A
CAGAGCTGGGGTCAGTCCTGTCCTCACGGCCCTGTGCGCCGCCGCCCCAGCTTGCAGGTCCCTCTGCCCCTAGGTTTCTGCGGTCCTGTGCCTGCAAGGGAGGTGGTCTCATCGTGTGAGGCTCTGC
ATAD3C
TGGGTCTCCCTTGGAGGGTGTGTGTGCCCTGGGGTGGGAGATGGAGACAAGTTTGCTCCCACGGGAAGTTGGACACCAGCAGGTCCTGTGTGTCGGGGCGGAACCTGGGACCTTGGTCCCCCGCCCG
ATAD3A
TGGGTCTCCCTTGGAGGGTGTGTGTGCCCTGGGGTGGGAGATGGAGACAAGTTTGCTCCCACGGGAAGTTGGACACCAGCAGGTCCTGTGTGTCGGGGCGGAACCTGGGACCTTGGTCCCCCGCCCG
ATAD3C
GATGCTGGCCAAGGGTGCACCCTCCAGGCTTGGGGCCCACCCGACTTTGTGTGGCCTCTGTGGGCTGCCGCCCAGATGTCCCCCATAGGGTGACCGCCCCATGGCCAGTCTCCCTAGTCCCTCCCAA
ATAD3A
GATGCTGGCCAAGGGTGCACCCTCCAGGCTTGGGGCCCACCCGACTTTGTGTGGCCTCTGTGGGCTGCCGCCCAGAGGTCCCCCATAGGGTGACCGCCCCATGGCCAGGCTCCCTAGTCCCTCCCAA
ATAD3C
GTCCCCTAATTTTGAGTTTTCTTGGTCTCCTGGGTCCCTCCAGCCCCAGTCACGTGTCACATGGAGGATCAAGTCCTGCTGGTCGGCCGTGGCTGACTCCTCAGGCACGTTGGGCTCCTGGGTCAGC
ATAD3A
GTCCCCTAATTTTGAGTTTTCTTGGTCTCCTGGGCCCCTCCAGCCCCAGTCACGTGTCACACGGAGGATCAAGTCCTGCTGGTCGGCCGTGGCTGACTCCTCAGGCACGTTGGGCTCCCAGGTCAGC
Duplication group d
P7
1:1395419
ATAD3C
TGCTGCCGGTAGACGCTCCCTGGAGCCCTGACTCGGGTCCTTCCCAGAGAGGCAAGGCTGGGGCCCTGCTGAGCCTCCAGTGAACCCGGGCCCCCGAGGTCCTGCTCCTGGCTCGCGTGGCAGTATT
ATAD3A
TGCTGCCGGTGGATGCTCCCTGGAGCCCTGACTCGGGTCCTTCCCAGAGAGGCAAGGCTGGGGCCCTGCTGAGCCTCCAGTGAACCCGGGCCCCTGAGGTCCTGCTCCTGGCACGTGTGGGCGAC--
1:1462718
ATAD3C
TTTTTTTTTTTTTTTTTGAGATGGAGTTTTTGCTTTTTCTGCCCAGGCTGAGGTGCAATGGCGTGATCTTGGCTCACTGCAACCTCCACCTCCTGGGTTCAAGC----------GATTCTCCTA
ATAD3A
----------TTCTCGACATGGA-------CT--------CCGGG----------TCCCGAATCCCTGCTCCCAGCACAG-CAGGGGTCAGGCAGCAGGAGAGAGTGGTGTTCCCG

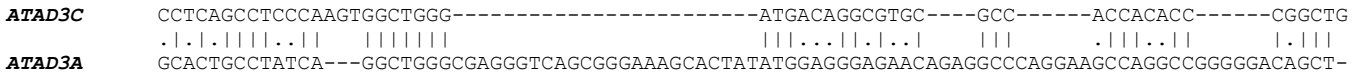
ATAD3C
CCTCAGCCTCCCAAGTGGCTGGG-----------------------ATGACAGGCGTGC----GCC------ACCACACC------CGGCTG
ATAD3A
GCACTGCCTATCA---GGCTGGGCGAGGGTCAGCGGGAAAGCACTATATGGAGGGAGAACAGAGGCCCAGGAAGCCAGGCCGGGGGACAGCT-

Supplemental Table 3. Analyses of mitochondrial respiratory chain enzymes and mtDNA in *ATAD3* duplication cohort, related to **Figure 4**.

Patient[a]	Cell / Tissue[a]	% Complex I[b]	% Complex II[b]	% Complex II+III[b]	% Complex III[b]	% Complex IV[b]	% Citrate Synthase[b]	% mtDNA/nDNA[c]
P2a	Fb							
	M	43	71	115	82	53	82	
	L	147	292		221	128	296	134
	H							
P3	Fb							
	M	124	144	172	132	119	124	
	L	91	320		310	146	387	
	H							
P4	Fb	17	171	104	169	105	129	
	M	14	47	41	27	22	44	
	L	58	243		345	58	364	469 ± 249
	H							
P5	Fb	65	215	90	88	79	118	
	M	17	49	72	50	59	56	
	L	44	121		108	69	221	85 ± 2
	H	6	129	125	95	76	104	
P6	Fb							
	M	5	16	20	21	20	38	19 ± 1
	L	12	111		28	42	293	181 ± 92
	H	3	64	86	60	23	117	
P7	Fb			57		49		
	M	22	38	242		41	48	
	L	16	51			85	275	
	H	5	45	30	80	50	84	
P8	Fb	76	144	146	87	133	129	
	M	363	204	322		136	211	
	L	13	192			99	396	77 ± 12
	H	6	132	54	294	124	116	

P9	Fb	93	190	167	198	120	147	
	M	22	51	61	45	39	62	
	L	42	193		83	56	429	
	H	1	135	70	52	62	149	
P10	Fb	87	85		113	60	117	
	M	25	48		32	11	55	32
	L	92	183		158	261	227	174
	H	7	139		142	46	128	14
P11	Fb	106	88		159	76	177	
	M	12	28		25	10	21	
	L	70	173		291	218	241	
	H	2	40		38	36	40	169
P12	Fb	82	72		123	58	80	
	M							
	L							
	H							
P13	Fb							
	M	70	170		97	78	101	
	L	16	84		40	56	151	
	H	2	240		244	32	111	
P14	Fb							
	M	84	134	165	156	125	134	
	L	8	350		244	93	391	134
	H							
P16	Fb							
	M	33	71	35	33	50	50	
	L							
	H							

[a]Diagnostic respiratory chain enzymology performed in patients with available tissues/cell lines. Fb, fibroblasts; M, skeletal muscle; L, liver; H, heart.

[b]Respiratory chain and citrate synthase enzymology values calculated as the % of control mean.

[c]mtDNA depletion results with indicated error values (SD) were performed as research studies rather than as part of clinical diagnostic molecular investigations.

Supplemental Table 4. PCR Primer sequences, related to **Figures 2** and **3**, **Supplemental Figure 2** and **Supplemental Table 2**.

Primer	Sequence	Orientation	Region of chromosome (hg19)	Gene[a]	Purpose
OT441[b]	5'-AGGACAAATGGAGCAACTTCG-3'	FWD	chr1:g.1,407,395-1,407,415 chr1:g.1,447,779-1,447,799	*ATAD3B* and *ATAD3A*	cDNA
OT443[b]	5'-CCTCCTCCCTCCTCTCTCAG-3'	REV	chr1:g.1,469,944-1,469,963	*ATAD3A*	cDNA
OT445[b]	5'-GCCCCACTTCTGTCTAGTCCT-3'	REV	chr1:g.1,431,422-1,431,442	*ATAD3B*	cDNA
OT453	5'-CACCCCTCTGTGGTTAAATCC-3'	REV	chr1:g.1,404,126-1,404,146	*ATAD3C*	cDNA
OT583	5'-CTGCACTCAGGCATGGACTA-3'	FWD	chr1:g.1,391,614-1,391,633 chr1:g.1,421,933-1,421,952 chr1:g.1,459,662-1,459,681	*ATAD3C*, *ATAD3B*, and *ATAD3A*	gDNA
OT864	5'-GCATCTCTTTAGCTCAGAAGTTCG-3'	REV	chr1:g.1,394,022-1,394,045	*ATAD3C*	gDNA
OT865	5'-TGCACAGTGTCTCCTCCAAACC-3'	FWD	chr1:g.1,459,180-1,459,201	*ATAD3A*	gDNA
OT866	5'-CAAGCTGGGTGAGAGTGATGCC-3'	REV	chr1:g.1,392,468-1,392,489	*ATAD3C*	gDNA
OT873	5'-TGGTCAGGCTTTTGAGAGTAGA-3'	FWD	chr1:g.1,461,700-1,461,721	*ATAD3A*	gDNA
OT879	5'-CTGTTCTCAGGTGGGGATGA-3'	REV	chr1:g.1,396,494-1,396,513	*ATAD3C*	gDNA
OT644[b]	5'-TGACGGAGGGCATGTCGG-3'	FWD	chr1:g.1,464,659-1,464,676 chr1:g.1,425,999-1,426,016	*ATAD3A* and *ATAD3B*	qRT-PCR
OT646[b]	5'-AGCACATCTTCTGCTGGTGC-3'	REV	chr1:g.1,469,383-1,469,402	*ATAD3A*	qRT-PCR
OT645[b]	5'-AGCGCATCTTCTGTCGGTAC-3'	REV	chr1:g.1,430,942-1,430,961	*ATAD3B*	qRT-PCR
ATAD3C-qRT-PCR-F	5'-TGACAGAGGGCATGTCAT-3'	FWD	chr1:g.1,398,036-1,398,053	*ATAD3C*	qRT-PCR
ATAD3C-qRT-PCR-R	5'-AGCGCATCATCTGCTGGTGC-3'	REV	chr1:g.1,403,841-1,403,860	*ATAD3C*	qRT-PCR
b-actin-rt-F	5'-GCGAGAAGATGACCCAGATC-3'	FWD	chr7:g.5,568,348-5,568,350/ chr7:g.5,568,792-5,568,808	*ACTB*	qRT-PCR
b-actin-rt-R	5'-GGATAGCACAGCCTGGATAG-3'	REV	chr7:g.5,568,291-5,568,310	*ACTB*	qRT-PCR

[a]Some of the DNA oligos are not specific and bind to several *ATAD3* regions, as indicated.

[b]Previously reported[19]

Supplemental Table 5. Proteomic data for protein analysis, related to **Figure 3** and **Supplemental Figures 4** and **5**.

Supplemental Table 6. Proteomic data for peptide analysis, related to **Figure 3** and **Supplemental Figure 4.**